NASA/TM–2015-218685

Characterization of Residual Stress Effects on Fatigue Crack Growth of a Friction Stir Welded Aluminum Alloy

John A. Newman and Stephen W. Smith
Langley Research Center, Hampton, Virginia

Banavara R. Seshadri
National Institute of Aerospace, Hampton, Virginia

Mark A. James, Richard L. Brazill, and Robert W. Schultz
Alcoa Technical Center, Acola Center, Pennsylvania

J. Keith Donald and Amy Blair
Fracture Technology Associates, Bethlehem, Pennsylvania

February 2015

NASA STI Program . . . in Profile

Since its founding, NASA has been dedicated to the advancement of aeronautics and space science. The NASA scientific and technical information (STI) program plays a key part in helping NASA maintain this important role.

The NASA STI program operates under the auspices of the Agency Chief Information Officer. It collects, organizes, provides for archiving, and disseminates NASA's STI. The NASA STI program provides access to the NTRS Registered and its public interface, the NASA Technical Reports Server, thus providing one of the largest collections of aeronautical and space science STI in the world. Results are published in both non-NASA channels and by NASA in the NASA STI Report Series, which includes the following report types:

- TECHNICAL PUBLICATION. Reports of completed research or a major significant phase of research that present the results of NASA Programs and include extensive data or theoretical analysis. Includes compilations of significant scientific and technical data and information deemed to be of continuing reference value. NASA counter-part of peer-reviewed formal professional papers but has less stringent limitations on manuscript length and extent of graphic presentations.

- TECHNICAL MEMORANDUM. Scientific and technical findings that are preliminary or of specialized interest, e.g., quick release reports, working papers, and bibliographies that contain minimal annotation. Does not contain extensive analysis.

- CONTRACTOR REPORT. Scientific and technical findings by NASA-sponsored contractors and grantees.

- CONFERENCE PUBLICATION. Collected papers from scientific and technical conferences, symposia, seminars, or other meetings sponsored or co-sponsored by NASA.

- SPECIAL PUBLICATION. Scientific, technical, or historical information from NASA programs, projects, and missions, often concerned with subjects having substantial public interest.

- TECHNICAL TRANSLATION. English-language translations of foreign scientific and technical material pertinent to NASA's mission.

Specialized services also include organizing and publishing research results, distributing specialized research announcements and feeds, providing information desk and personal search support, and enabling data exchange services.

For more information about the NASA STI program, see the following:

- Access the NASA STI program home page at http://www.sti.nasa.gov

- E-mail your question to help@sti.nasa.gov

- Phone the NASA STI Information Desk at 757-864-9658

- Write to:
  NASA STI Information Desk
  Mail Stop 148
  NASA Langley Research Center
  Hampton, VA 23681-2199

NASA/TM–2015-218685

Characterization of Residual Stress Effects on Fatigue Crack Growth of a Friction Stir Welded Aluminum Alloy

John A. New and Stephen W. Smith
Langley Research Center, Hampton, Virginia

Banavara R. Seshadri
National Institute of Aerospace, Hampton, Virginia

Mark A. James, Richard L. Brazill, and Robert W. Schultz
Alcoa Technical Center, Acola Center, Pennsylvania

J. Keith Donald and Amy Blair
Fracture Technology Associates, Bethlehem, Pennsylvania

National Aeronautics and
Space Administration

Langley Research Center
Hampton, Virginia 23681-2199

February 2015

Available from:

NASA STI Program / Mail Stop 148
NASA Langley Research Center
Hampton, VA 23681-2199
Fax: 757-864-6500

Abstract

An on-line compliance-based method to account for residual stress effects in stress-intensity factor and fatigue crack growth property determinations has been evaluated. Residual stress-intensity factor results determined from specimens containing friction stir weld induced residual stresses are presented, and the on-line method results were found to be in excellent agreement with residual stress-intensity factor data obtained using the cut-compliance method. Variable stress-intensity factor tests were designed to demonstrate that a simple superposition model, summing the applied stress-intensity factor with the residual stress-intensity factor, can be used to determine the total crack-tip stress-intensity factor. Finite element, VCCT (virtual crack closure technique), and J-integral analysis methods have been used to characterize weld-induced residual stress using thermal expansion/contraction in the form of an equivalent ΔT (change in local temperature during welding) to simulate the welding process. This equivalent ΔT was established and applied to analyze different specimen configurations to predict residual stress distributions and associated residual stress-intensity factor values. The predictions were found to agree well with experimental results obtained using the crack- and cut-compliance methods.

Introduction

The increased use of integral structures has been identified as critical for the development of improved aerospace structures [1]. Integral structures reduce the use of rivets and the need to create lap joints, the primary sources for the initiation of multi-site fatigue damage in airframe structures [2]. Additionally, the replacement of traditional riveting approaches permits modular fabrication of large sections of the airframe, which can result in reduced construction time, cost and weight. One primary method being examined to produce and join large modular sections of aluminum structure is solid state welding. Of particular interest to the aerospace industry is the use of friction stir welding (FSW), a solid-state process well suited for joining aluminum alloys. However, the residual stresses that result from FSW create complex crack propagation challenges, making it difficult to make accurate fatigue life predictions. This paper will explore a method to quantify residual stress for welded materials and explain how this information can be used to improve fatigue life predictions. Results are presented from multiple laboratories – NASA Langley Research Center (herein referred to as LaRC), Alcoa Technical Center (Alcoa), and Fracture Technologies Associates (FTA) – to show repeatability of results.

Although friction stir welding is a solid-state process (meaning that it does not result in the local melting of material), there is sufficient heating and mechanical work to result in residual stress within welded components. The residual stress distribution about a friction stir weld in aluminum alloy (AA) 2024-T351 was characterized utilizing a hole-drilling method [3]. In this study, a tensile residual stress was observed along the centerline and a steep residual stress gradient existed perpendicular to the weld direction. Near the edge of the weld nugget, the residual stress was observed to decrease rapidly, becoming compressive and approaching zero further away from the nugget. Parallel to the weld direction, little change in the residual stress

was observed, suggesting a consistent process as the weld advances. In addition to residual stress gradients, gradients of hardness and microstructure, specifically grain size, were also observed [3].

A tensile residual stress normal to a growing crack path will result in increased crack growth rates, while a compressive residual stress can dramatically reduce crack growth rates due to crack closure, even resulting in crack arrest [3-5]. In a weldment, which can exhibit large variations in residual stress as well as microstructure, residual stress has been shown to affect crack growth rates to a greater extent than the microstructural variations [3, 6-8].

The development of accurate fatigue life predictions requires the generation of appropriate fatigue crack growth rate data using mechanical test specimens. However, when a mechanical test specimen is extracted from a structure or a larger product containing residual stress, the residual stress will redistribute, resulting in a residual stress field in the test specimen that is very different from that within the structure [9]. Since residual stress can have a profound effect on fatigue crack growth [6-8], the use of data generated from a test specimen may not be appropriate to predict structural fatigue life. Further complicating this issue is the fact that the residual stress in a cracked body redistributes as the crack propagates, resulting in a variable effect [9]. This crack-induced residual stress redistribution will be different for a test specimen (depending upon the type of loading) than for a structure, particularly if the crack path simulated in the test specimen is not consistent with that produced for an in-service structure.

In the examples described above, the residual stress is thought to bias both the property determination and the structural response. A more rigorous approach is to properly account for the residual stress effects on the crack driving force in both the property determination and the structural evaluation – that is, to separate the residual stress effects from the specimen during property determination for true fatigue crack growth (FCG) property data and to reintroduce the appropriate residual stress effects in the structural evaluation. As noted, the residual stress in a coupon excised from a structure will have different residual stress than the structure due to redistribution (from coupon removal), and crack growth testing likely also causes redistribution in the coupon. Other methods could be applied where the residual stress is measured in the specimen and then combined with analysis to evaluate efficacy; however, most methods are either destructive (e.g. slitting, hole drilling, etc.) and thus affect the residual stress distribution or are difficult to apply and costly for bulk residual stress in aluminum alloy materials (e.g. neutron diffraction).

This paper demonstrates a new in-situ test method [10] for the measurement of residual stress-intensity factor at a crack tip during fatigue crack growth rate testing. The method shows great promise as a tool for partitioning the residual stress effects that occur during FCG testing on common specimens such as the compact or middle tension specimens. In combination with the new test method, the paper outlines a computational methodology that could be applied to quantify the residual stress distribution and fatigue life performance of a welded structure using the data obtained from a test specimen. Much of this work was presented at the Residual Stress Summit 2010 [11]. The experimental work presented here is similar to that subsequently studied by Olson and Hill [12].

Use of Compliance to Experimentally Determine Residual Stress-Intensity Factor

Compliance is a relationship of displacement at some location on a mechanical test specimen as a function of applied force and is a versatile tool for fatigue and fracture testing.

Compliance-based measurements have been used to determine crack length [13] and closure loads [14, 15]. In this paper, the crack-compliance method [10] is demonstrated as a viable approach to determine the residual stress-intensity factor as a function of crack extension.

Figure 1 is a schematic of a load-versus-displacement curve that represents compliance change during crack growth. Nonlinear effects such as crack closure have been omitted for clarity. As a crack grows in a residual stfor the ress free body, the compliance increases, but the displacements at zero load always return to the same value, as indicated in Figure 1. However, when the body has residual stress, the body load is redistributed as the crack grows, and this redistribution is reflected in a displacement translation, which in the sketch appears as a $\Delta\delta_{res}$ shift to the right denoting residual stress presence that acts to open the crack. Donald and Lados [10] showed that as a crack propagates through a residual stress field, there is a non-proportional effect as residual stresses are relieved, resulting in a shift of the load-versus-displacement curve, $\Delta\delta_{residual}$ (also illustrated in Figure 1). (Note that if crack closure is influencing the compliance data, the slope of the elastic portion of the load displacement curves (above the crack opening load) must be used.) Donald and Lados [10] showed that the residual stress-intensity factor during this increment of crack growth can be expressed as,

$$K_{residual} = K_{max}\left(\frac{\Delta\delta_{residual}}{\Delta\delta_{max}}\right),$$

where K_{max} is the maximum applied stress-intensity factor, $K_{residual}$ is the residual stress-intensity factor, $\Delta\delta_{residual}$ is the shift in the crack opening displacement due to non-proportional residual stress effects, and $\Delta\delta_{max}$ is the change in crack opening displacement due to crack growth. A more complete discussion of this method is given elsewhere [10].

Use of Computational Methods for Residual Stress Modeling

Computational methods have an essential role for integrating residual stress into a structural analysis because residual stress measurements are complex, expensive, and most importantly, usually limited to selected locations in a component. Often measurements are simply not feasible at critical locations of interest. As a result, a viable strategy for design analysis with residual stress is to use experiments to validate a residual stress model at selected locations in a component and in related components, then to use the validated model to predict the residual stress at the locations of interest for the component.

A variety of computational methods have been developed to estimate residual stress effects in structures. Broadly, the methods can be broken down into methods for estimating the residual stress in the body and methods for estimating the stress-intensity factor for a crack in a residual stress field. Some techniques have been developed using the weight function method [16, 17], or finite element analysis using the least squares technique [18-20]. Previous efforts on this topic have focused on importing experimentally-determined residual stress data into FEM models [19, 20]. Neutron diffraction has been used for measurement of residual stresses in various types of materials [21] and specimen types [22, 23], and Liljedahl, et al., [22-24] used the neutron diffraction method and FEM to characterize the residual stresses in a welded aluminum alloy. The stress distribution was measured using the neutron diffraction technique which was input into the FE model as initial stress and allowed to equilibrate.

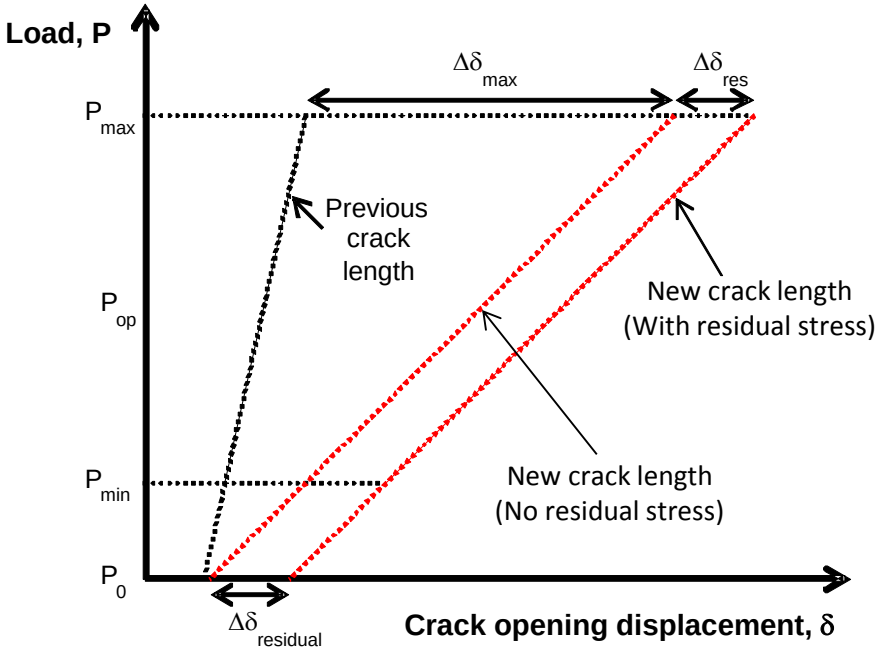

Figure 1. Schematic of displacement data used for the crack-compliance method to determine residual stress.

The approach used here is often called the inherent strain method (also called Eigen-strain method) and was outlined by Hill and Nelson and others [25, 26, 27]. A similar approach was outlined by Liljedahl [22-24] to determine weld-induced residual stresses.

Equivalent thermal loads are evaluated by defining initial strain due to welding along the length/width of the weld region. Using the elastic modulus, E, coefficient of thermal expansion, α, and change in temperature, ΔT, equivalent thermal loads are calculated to produce the residual stress field. Conceptually, the residual stress field is determined by modeling the heating of the entire weldment volume to some temperature and then cooling to room temperature. The temperature change, ΔT, is calibrated by comparing the predicted residual stress field to that measured for coupon test data. For a specific combination of material type and welding process, the same ΔT may be used to predict the residual stress field for other configurations (specimen type, component, or panel size and shape) that contains a weld produced in the same manner as that used to calibrate the value of ΔT. Note that a variety of limitations exist. The conceptual model assumes that the temperature history and cooling rates as well as the transient material response are equivalent for the original calibrated case and the predicted case. For instance, if the structural heat capacity is different due to the size of the structure, then the cooling rates could be different, which could affect the residual stress calibration. However, this simple linear elastic cooling model has worked well for many cases. In the current work, rather than directly comparing computational results to the residual stress field, the authors compare model-based calculated stress-intensity factor results with the experimentally determined $K_{residual}$ value (stress-intensity factor due to residual stress loading) as a function of crack length. Thus, the residual stress prediction is implicitly validated and the concept of residual stress-intensity factor and effect of stress redistribution with crack growth are validated directly.

Experimental Test Methods

To examine the residual stress produced from friction stir welding, an AA2024-T351 plate was sectioned into three pieces and two butt welds were produced to create a single piece containing two parallel welds. The plate was initially 1 inch thick, but 0.25 inch was removed from both the top and bottom faces prior to welding, reducing the weld nugget size and satisfying the limitations for the FSW machine used in this study. Subsequent to welding, an additional 0.125 inch was removed from both the top and bottom faces to produce a more uniform through-the-thickness weld configuration in the welded plate (see Figure 2). Standard compact (C(T)) specimens, having width and thickness dimensions of 4.0 inches and 0.25 inch, respectively, were machined from the welded plate in the T-L orientation (loading in the long transverse direction and crack growth in the longitudinal direction), as shown in Figure 3a. Three configurations of specimens were machined from the AA2024-T351 material. Two of these configurations were machined such that the weld was in a different location within the specimen (see Figure 3b). Specifically, one configuration was designed such that the crack growth would initially occur in a tensile-dominated residual stress field and the other in a compressive-dominated residual stress field. The third configuration was machined from the base AA2024-T351 material and contained no weld. Note that only the component of residual stress normal to the crack plane (perpendicular to the loading direction) are used to characterize specimens as being either tensile-dominated or compression-dominated. While this approach seems reasonable for the relatively simple geometry considered, the effect of the full stress tensor should be considered in general [28].

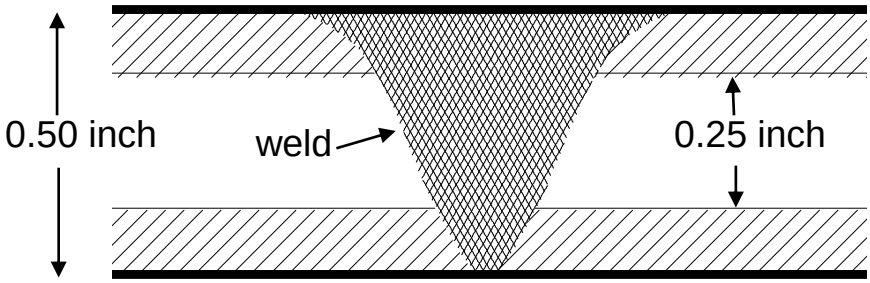

Figure 2. Through-the-thickness schematic of FSW material.

Residual Stress-Intensity Factor Determination

A variety of techniques are documented in the literature to quantify residual stresses where the part being examined is altered by cutting, drilling, or some other destructive process [29-33]. In the current study, the cut-compliance method will be used because it produces data that can easily be transformed to calculate the residual stress-intensity factor of interest for this work. The results from this method will be compared to the new crack-compliance approach that is being evaluated in this study [10].

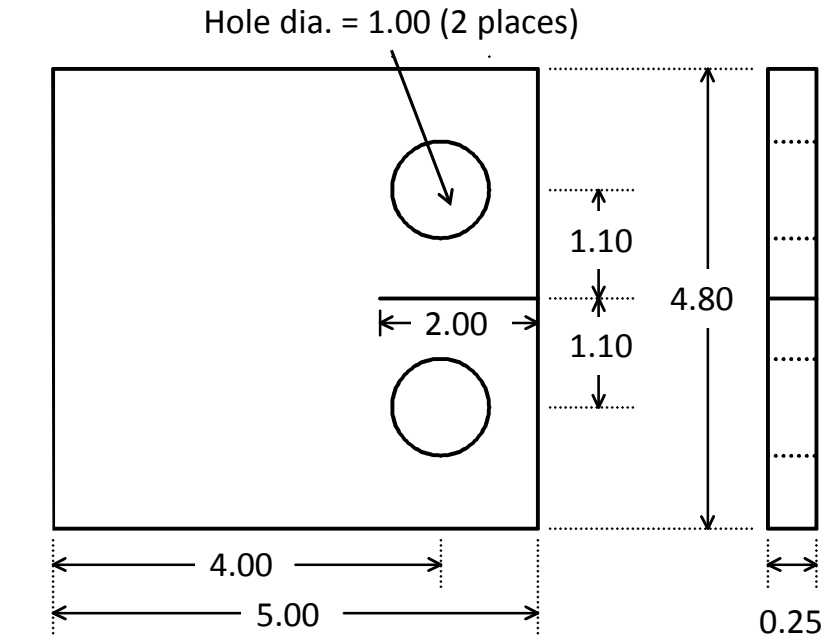

(a)

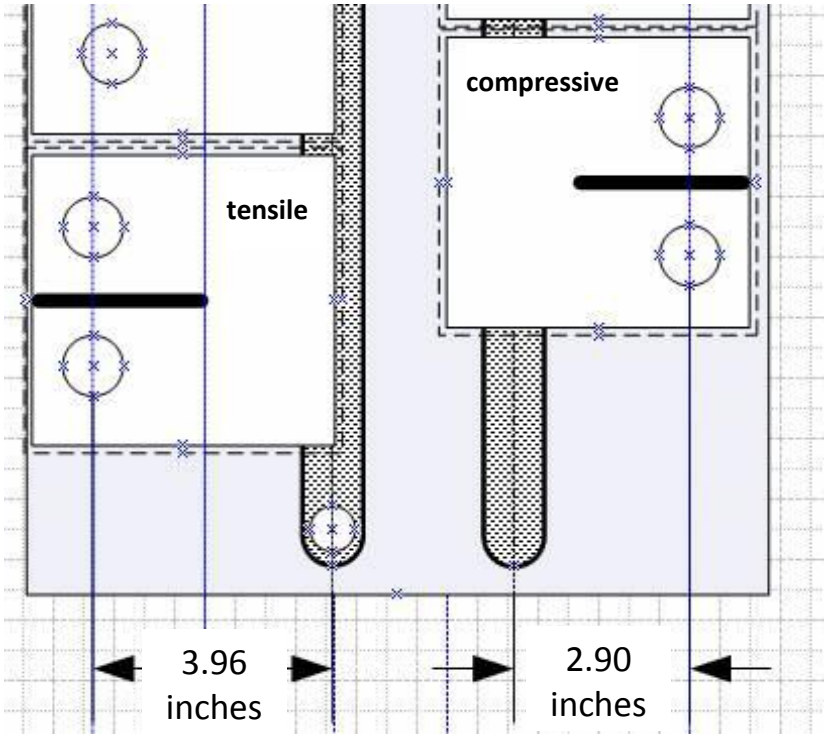

(b)

Figure 3. (a) Schematic of the compact tension specimen configuration used for this study. (b) The FSW location within two specimen configurations are shown. All dimensions shown are in inches.

Cut-compliance Method

The cut-compliance method is described in detail elsewhere [29, 30], but is outlined here for convenience. Typically, specimens are cut (in a series of small increments) from the edge of the specimen along the direction of interest, which in this case is the anticipated crack growth direction for the C(T) specimens. After each cut increment, the change in strain is measured at predetermined locations. In the simplest case using Schindler's method [29], the strain is measured at the specimen back-face, and the residual stress-intensity factor is calculated directly from the measured strain gradient without explicitly calculating the residual stress field. Prime [30] outlines additional methods where the residual stress is calculated and then the residual stress-intensity is calculated from the residual stress field, and the strain gages need not be at the specimen back face (to increase strain measurement sensitivity). For the current work, the strains were converted to the residual stress-intensity factor using Schindler's method [29]. The typical cut increment was 0.078 inches, and a wire electrical discharge machining (EDM) process was used to produce the cut to minimize the potential for mechanical forces imparted on the specimen. Cut-compliance measurements were performed on specimens of the same overall dimensions and orientation as the C(T) specimens used for FCG testing (including pre-machined holes) but did not contain a pre-machined notch.

Crack-compliance Method

The crack-compliance method is similar to the cut-compliance method, but new surface area is created via fatigue loading and fatigue crack growth rather than EDM slitting [10]. Here, compliance data are measured to determine crack length and the residual stress-intensity factor during automated fatigue crack growth (FCG) testing as described above. The crack-compliance method has the advantage of producing both residual stress-intensity factor data and crack growth data simultaneously. The method works equally well with either front-face clip-gage-based compliance or with back-face strain-gage-based compliance.

Fatigue Crack Growth Rate Testing

Fatigue crack growth rate testing, in accordance with ASTM standard E 647 [13], was performed on specimens with and without friction stir welds. All fatigue crack growth rate tests were performed utilizing computer-controlled servo-hydraulic load frames. A front-face clip gage was monitored during fatigue loading and the compliance data are analyzed to determine crack length and residual stress-intensity factor. The applied force was modified as a function of crack length to control the applied stress-intensity factor, which is also known as K-control testing. This allows a constant cyclic stress-intensity factor, constant-ΔK, or a pre-determined variable-ΔK to be applied to the specimen.

The ASTM E 647 test standard does not have provisions for residual stress, and as a result, assumes that the total crack-tip stress-intensity factor is equal to the applied stress-intensity factor. However, in the current work it is necessary to distinguish between applied, residual and actual crack-tip stress-intensity factors. For the purposes of this paper the following convention is used: "Applied" stress-intensity factor is the value calculated from the E 647 equations based on the applied force. "Residual" stress-intensity factor is the value due to residual stress. "Tip" stress-intensity factor is the total value at the crack tip due to all body stresses acting on the crack (residual and applied).

Constant Applied ΔK Testing

Fatigue crack growth tests were performed under constant applied-ΔK conditions. When the resulting test data are plotted as crack length versus cycle count, the slope of these data is the crack growth rate, d*a*/dN. Constant applied-ΔK test results for compression-dominated and tensile-dominated specimens are shown in Figure 4, plotted as crack growth rate (d*a*/dN) versus crack length (*a*). In the absence of a residual stress field, the d*a*/dN would be expected to remain constant; however, the variable growth rates presented in Figure 4 are a direct result of residual stress.

The tensile-dominated data plotted in Figure 4 were generated at applied $\Delta K = 13.5$ ksi$\sqrt{in}$ and a load ratio of R = 0.1[1]. The crack growth rate from the crack starter notch (approximately 1.0 inch long) was nearly constant (d*a*/dN approximately 1×10^{-5} inches/cycle) until reaching a crack length of nearly 2.5 inches. As the crack approached the weld (starting at a crack length of approximately 2.8 inches), the crack growth rate decreased as $K_{residual}$ became compressive. The minimum value in d*a*/dN (approximately 10^{-7} inches/cycle) occurred at a crack length of nearly 3.1 inches, suggesting a maximum compressive $K_{residual}$ at that crack length.

The compression-dominated data plotted in Figure 4 were started at applied $\Delta K = 9.0$ ksi$\sqrt{in}$ and R = 0.1. The crack growth rate from the crack starter notch (approximately 1.0 inch long) was approximately d*a*/dN = 3×10^{-6} inches/cycle, but rapidly decreased until crack arrest occurred at a crack length of nearly 1.5 inches. The applied loading was increased to obtain applied $\Delta K = 13.5$ ksi$\sqrt{in}$ (R = 0.1) which permitted an additional 0.25 inch of crack propagation before crack arrest occurred again. This behavior suggests that the crack is growing within an increasingly compressive residual stress field as the crack propagates.

Residual stress-intensity factor data for the tensile-dominated and compression-dominated specimen configurations are shown as Figures 5a and 5b, respectively. Testing was conducted by three laboratories (Alcoa, LaRC, and FTA) as indicated in the legend. Cut-compliance test results (performed at Alcoa) are shown as lines, and crack-compliance test results (performed at LaRC and FTA) are shown as symbols. Here, results are presented as the residual stress-intensity factor, $K_{residual}$, using the procedures described previously. Excellent agreement is observed between all sets of data, suggesting that the experimentally obtained residual stress-intensity factor values are independent of test method or laboratory.

As seen in Figure 5a, the tensile-dominated residual stresses are nearly zero at zero crack length (coinciding with the centerline of the pin holes) and gradually increase to a maximum $K_{residual}$ value of approximately 10 ksi$\sqrt{in}$ (tensile) near a crack length of 1.75 inches. $K_{residual}$ decreases with further increase in crack/cut length to a minimum value of nearly -10 ksi$\sqrt{in}$ (compressive) near a crack length of 3.0 inches. The decreasing residual stress-intensity factor values are consistent with the crack length interval in which d*a*/dN is observed to decrease in the tensile-dominated specimen presented in Figure 4. As the crack (or cut) reaches the edge of the weld (at a crack/cut length of approximately 3.5 inches), the $K_{residual}$ is nearly zero.

---

[1] The load ratio, R, is defined as the ratio of the minimum to maximum values of applied load (P_{min}/P_{max}).

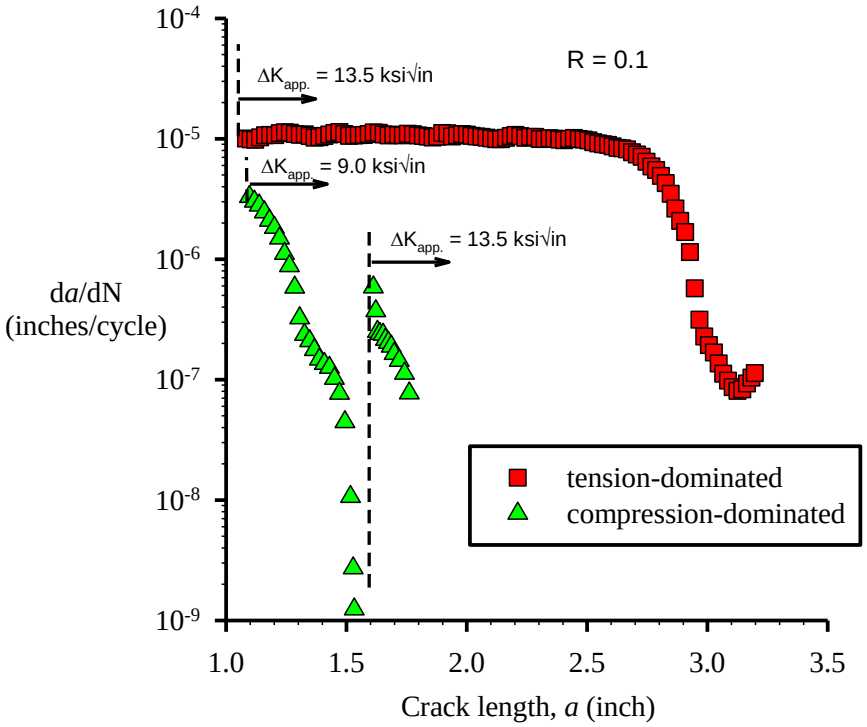

Figure 4 – Fatigue crack growth rate versus crack length for constant-ΔK tests of tensile and compressive-dominated C(T) specimens. Data were generated at NASA Langley Research Center.

The $K_{residual}$ profile for the compression-dominated specimen (Figure 5b) is nearly zero at zero crack length, and gradually decreases (increasing compressive stress) with increasing crack length. The greatest value of $K_{residual}$ is approximately -20 ksi√in (compressive), occurring near a crack length of 2.1 inches. The edge of the weld is at a crack/cut length of approximately 2.3 inches. As the crack/cut progresses across the weld, the $K_{residual}$ values become less compressive and eventually become tensile as the crack/cut exits the weld at a crack length of approximately 3.3 inches. At this point in the tests, the crack-compliance and cut-compliance tests diverge, presumably due to the crack-tip plastic zone approaching the size of the remaining ligament on the specimen resulting in linear-elastic fracture mechanics being invalid. Note that both the cut-compliance and crack-compliance methods are subject to linear elasticity limitations. However, the crack-compliance method seems to be more prone to plasticity in this circumstance. It may be that the finite applied loads of the crack-compliance method create increasing plasticity effects in the small remaining specimen ligament as the crack tip approaches the back face of the specimen. The cut-compliance specimen has no externally applied loads, and as the ligament becomes small, the residual stress is relaxed to zero minimizing the plasticity effects.

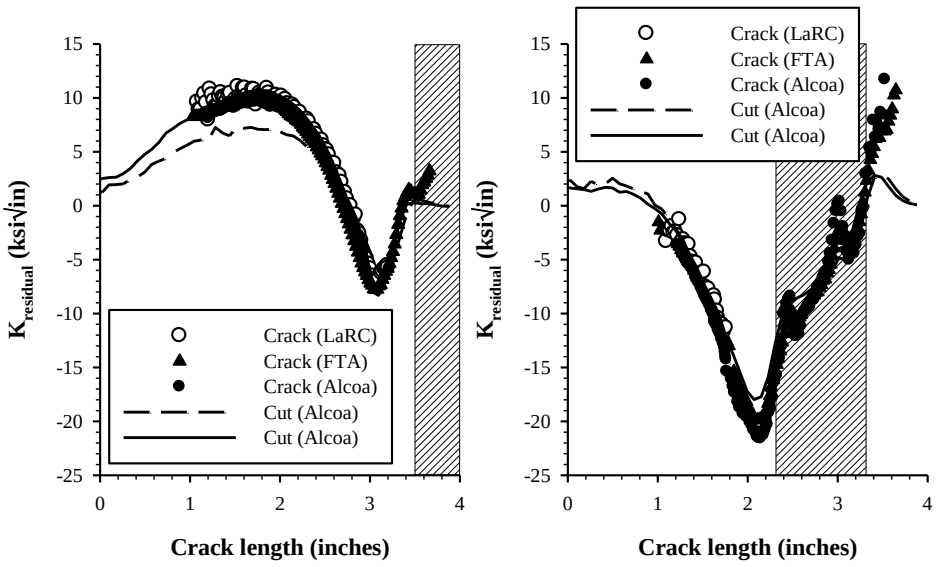

(a) Tensile-dominated (b) Compression-dominated

Figure 5 – Experimental results from cut-compliance and crack-compliance test methods.

Constant Crack-Tip ΔK Testing

Additional FCG testing was conducted to determine the effect of linear elastic superposition of the applied and residual stress-intensity factor. Using the premise that total crack-tip loading is a superposition of a non-cyclic $K_{residual}$ (recall Figure 5) onto the applied cyclic loading; tests were designed to maintain a constant cyclic crack-tip stress-intensity factor. Presumably, a constant crack growth rate, d*a*/dN, can be maintained by compensating for the mean stress effect induced by the residual stresses. Based on the $K_{residual}$ profile of Figure 5a, a variable $K_{applied}$ test was designed to achieve a constant-ΔK_{tip} state for the tensile-dominated specimen. The K_{max} and R required to produce a constant-ΔK_{tip} = 9 ksi$\sqrt{}$in at R = 0.55 are plotted in Figures 6a and 6b, respectively. In a similar manner, a constant-ΔK_{tip} = 6.75 ksi$\sqrt{}$in at R = 0.55 test was designed for compressive-dominated specimens and the corresponding K_{max} and R values are plotted in Figures 7a and 7b, respectively. The applied ΔK and R values were selected to insure that the applied K_{max} would always be less than the fracture toughness of the base material.

The fatigue crack growth rate data for tensile-dominated and compression-dominated specimens are plotted in Figures 8a and 8b, respectively, as crack length versus cycle count. A constant slope of these data corresponds to a constant crack growth rate. During the test of the tensile-dominated specimen, the crack growth rate remains nearly constant as the crack propagated across the entire specimen. A slight deviation in crack growth rate was observed at a crack length greater than 3.0 inches (note, the deviation from the dotted line in Figure 8a), possibly a result of local changes in the material microstructure and yield strength near the weld. The deviation from a constant FCG rate in Figure 8a corresponds to the largest gradients in the residual stress-intensity factor (Figure 5a). However, the change in growth rate is much less than those observed for the applied constant-ΔK tests for the tensile-dominated specimen (Figure 4), suggesting that the effect of residual stress is much greater than any effect due to variation in material microstructure.

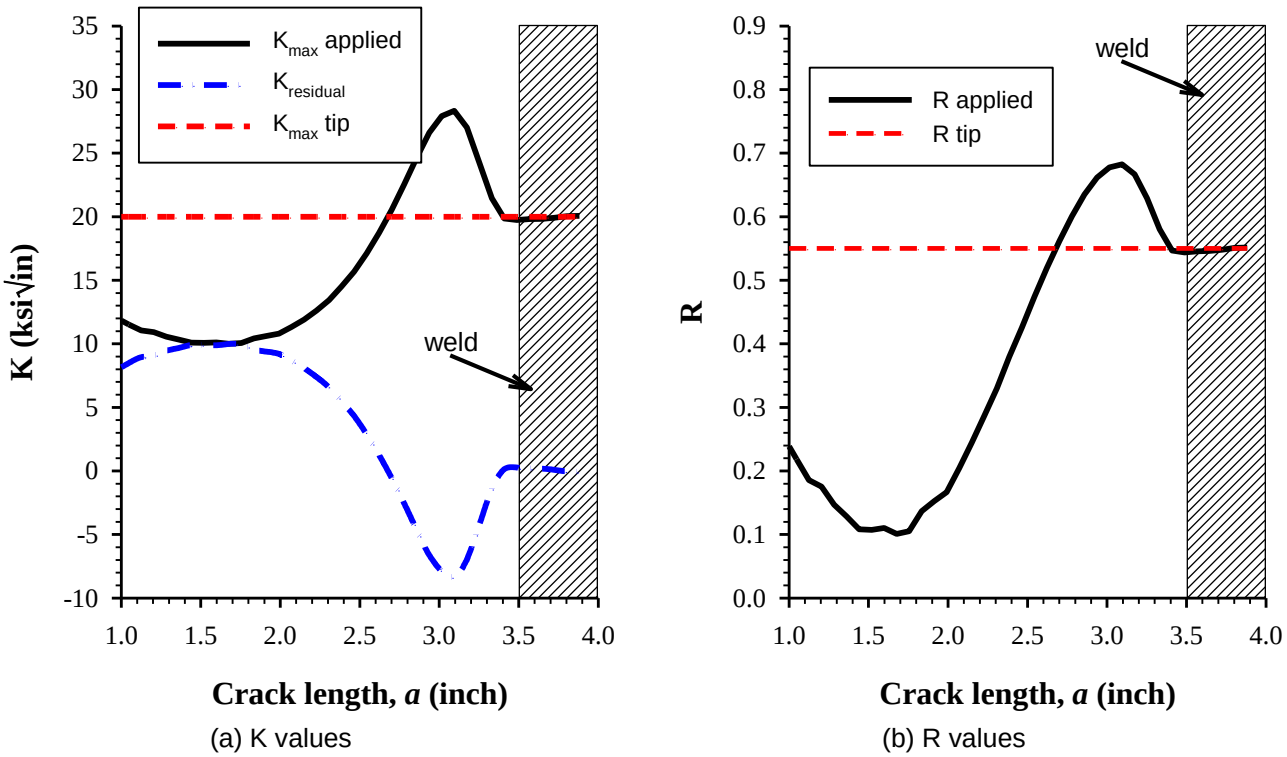

(a) K values (b) R values

Figure 6 – K and R values needed to maintain constant ΔK_{tip} = 9 ksi√in and R_{tip} = 0.55 for tensile-dominated specimens.

For the constant-ΔK_{tip} test on the compression-dominated specimen (Figure 8b), a nearly constant crack growth rate is observed up to a crack length of approximately 2.4 inches, which is nearly the same crack length as that corresponding to the peak applied loads. After this point in the test, a significant amount of crack closure was observed, likely causing the reduction in crack growth rate (slope of the curve).

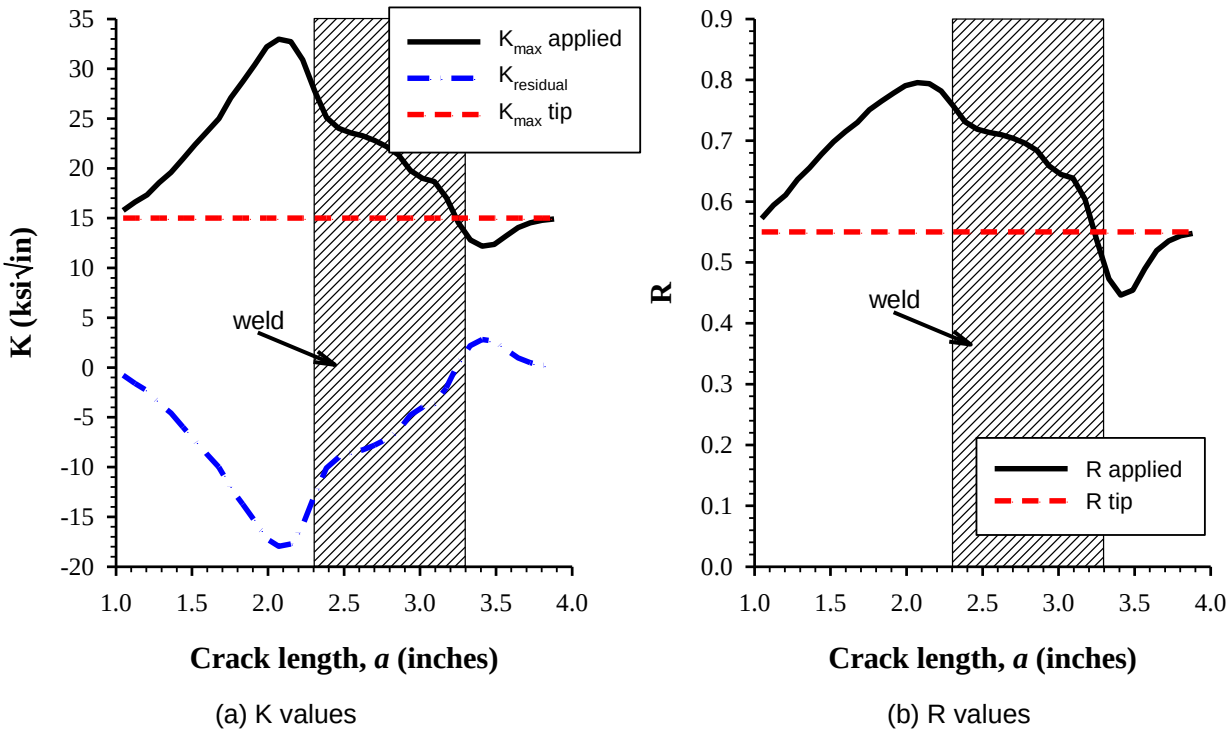

(a) K values (b) R values

Figure 7 – K and R values needed to maintain constant ΔK_{tip} = 6.75 ksi√in and R_{tip} = 0.55 for compression-dominated specimens.

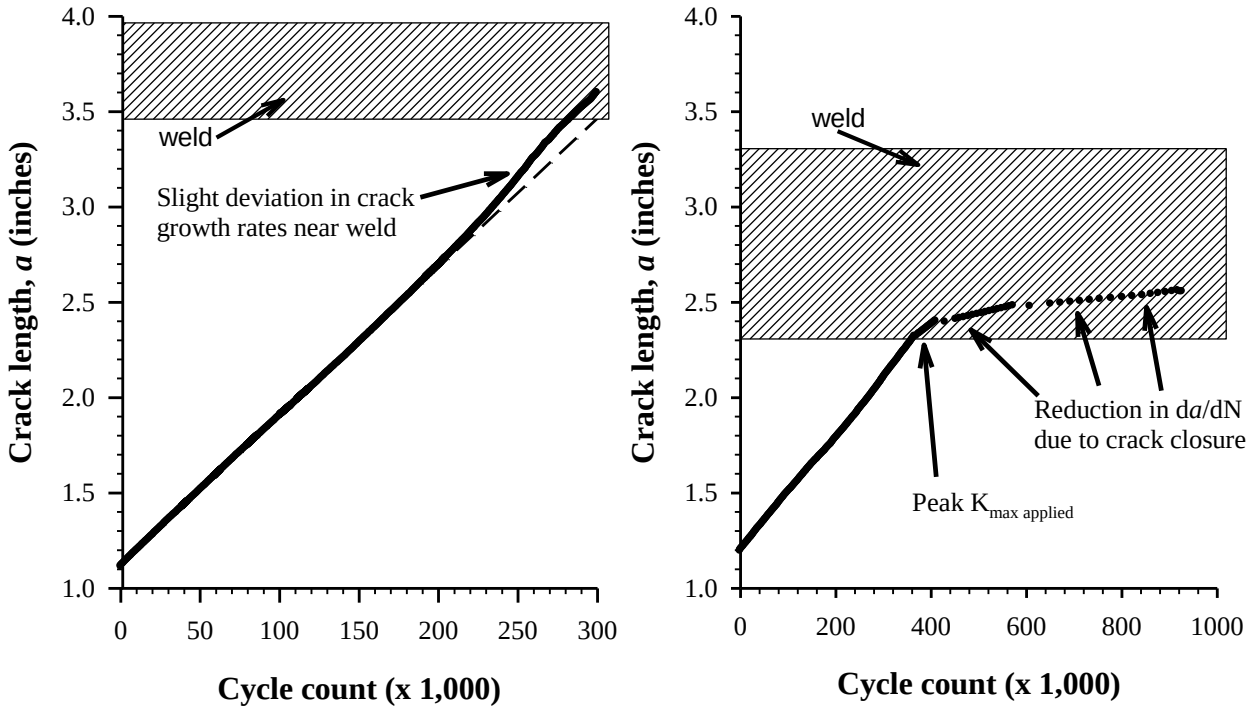

(a) Tensile-dominated specimen (b) Compressive-dominated specimen

Figure 8 – Crack length versus cycle count data for Constant-K_{tip} condition tests.

The crack growth rates obtained for the tensile-dominated specimen (Figure 8a; 1.25 inches < *a* < 2.30 inches) and the compression-dominated specimen (Figure 8b; 1.25 inches < *a* < 2.75 inches), are compared with constant-R = 0.55 FCG data for the base material (no weld; nominally free of residual stresses) in Figure 9. FCG testing of the base material was done in accordance with ASTM standard E647 [13], using a ΔK-reduction (C = -2/inch) for applied ΔK < 6.75 ksi√in, and a ΔK-increasing test (C = +5/inch) for applied ΔK > 6.75 ksi√in. Excellent agreement is observed between the base material results (open symbols) and the constant-ΔK_{tip} data (closed triangular symbols). This observation suggests that residual stresses affect the crack-tip stress state as a superimposed non-cyclic component that acts similar to a mean stress, $K_{tip} = K_{applied} + K_{residual}$.

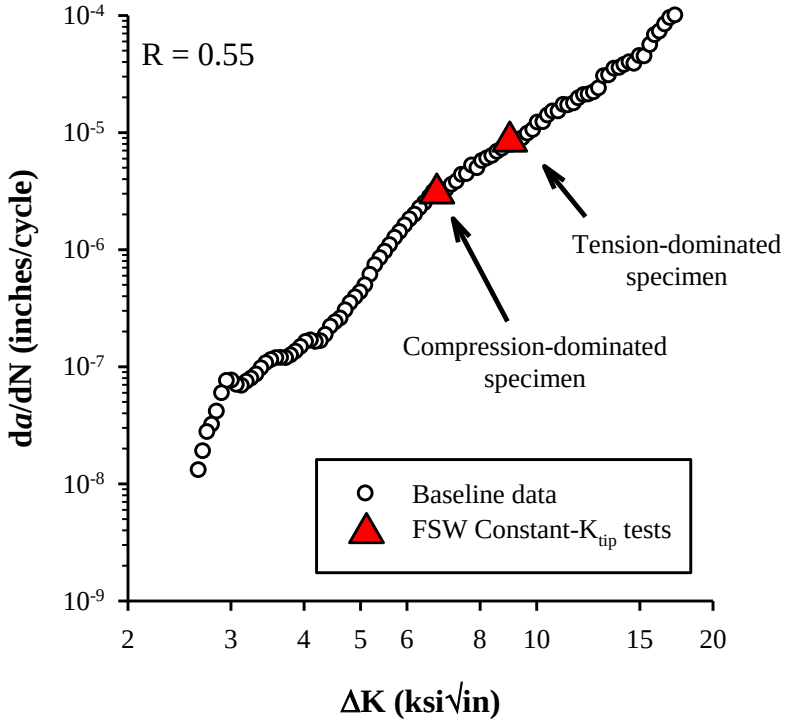

Figure 9 – Comparison of constant-ΔK_{tip} fatigue crack growth rate data for tensile and compressive-dominated specimens with FCG data for baseline specimen.

Computational Study

Computational results are compared with experimental data from both cut-compliance (Alcoa) and crack-compliance (LaRC, Alcoa, and FTA). Here, the cut and crack-compliance methods produce a $K_{residual}$ profile as a crack grows, while the thermal load method results in a profile of residual stress for an uncracked body. Therefore, it is necessary to perform a numerical simulation to determine the resultant $K_{residual}$ for a growing crack in the estimated residual stress field, or alternatively, to determine the residual stress field that would produce the $K_{residual}$ profile measured using the cut- and crack-compliance methods.

Stress-intensity factors were calculated using the virtual crack closure technique (VCCT) [34-36] and J-integral [37] methods. The virtual crack closure technique was proposed for 2D crack

configuration by Rybicki and Kanninen [34] and was extended to three dimensions (3D-VCCT) by Shivakumar, et al., [35]. The J-integral represents a way to calculate the strain energy release rate, or work (energy) per unit fracture surface area, in a material. The theoretical concept of J-integral was developed by Rice [37] who showed that an energetic contour path was independent of the path around a crack. In the current study, both the J-integral and 3D-VCCT techniques have been used to generate residual stress-intensity factor solutions [36].

Compact (C(T)) specimens exhibit two planes of symmetry, and consequently, only one fourth of the geometry is used for modeling. Iso-parametric eight-node brick elements were used in the model. All analyses were for 0.25 inch thick specimens. The width of the C(T) specimen is 4.0 inches measured from the centerline of the loading holes. The C(T) finite element analysis (FEA) model consisted of a total of 3,270 nodes and 1,516 brick elements. A typical finite element model of the C(T) specimen is shown in Figure 10 where the red shaded elements correspond to the weldment. AA2024-T3 was considered for all analyses with modulus E = 10,000 ksi (assumed linear-elastic deformation response) and coefficient of thermal expansion, α = 13.0x10^{-6} in/in^{o}F. The change in ΔT, from the welding temperature to room temperature, was first estimated and a residual stress distribution was determined. Three dimensional finite element simulations were then performed. The residual stress profile along the symmetry plane for tensile dominated C(T) specimen was then compared to the results obtained from the experimental methods and ΔT was modified until sufficiently reasonable agreement was obtained. The change in temperature, ΔT, in the weld zone due to the friction stir weld process was empirically estimated to be -200^{o}F, by fitting the predicted residual stress profile distribution to the experimentally measured values for the tensile-dominated configuration. Note that the value of ΔT is negative as the weldment is at an elevated temperature during the processing, and the residual stress is a result of the weldment being cooled to room temperature. This same value of ΔT was then applied to the analysis of the compressive-dominated specimen and the prediction results presented.

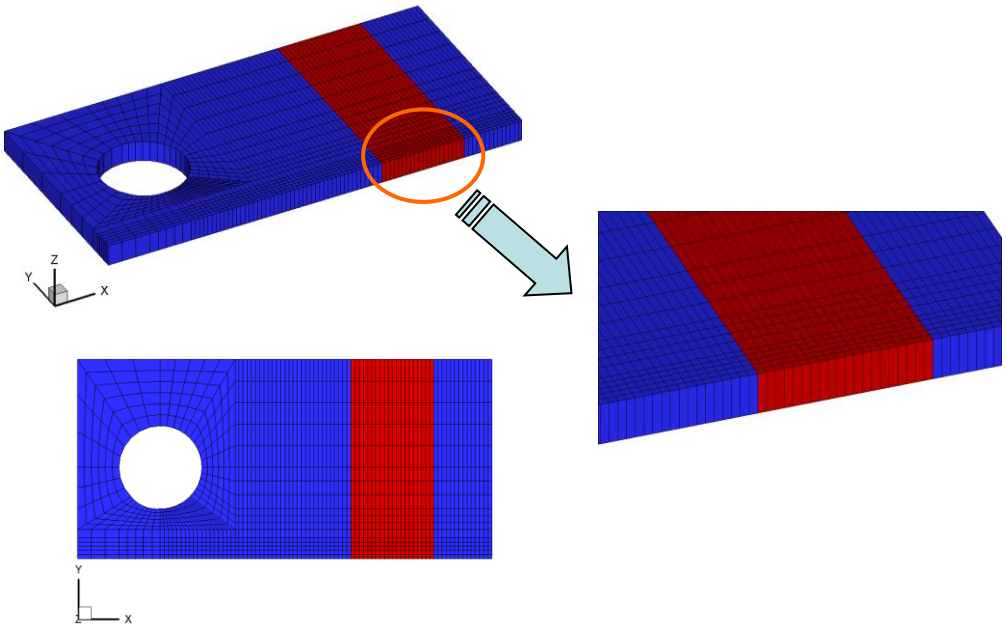

Figure 10 – A typical finite element mesh for 4 inch wide C(T) specimen.

Crack growth simulations were then performed with crack increments of 0.4 inch. The $K_{residual}$ at each increment was determined using VCCT technique [36, 37]. The calculated $K_{residual}$ profile was then compared to the results from the experimental methods. For the two weld locations (tensile-dominated and compression-dominated), $K_{residual}$ solutions were generated using the J-integral and 3D-VCCT techniques [36, 37], and are shown in Figures 11 and 12. Both crack-compliance and cut-compliance experimental data are shown for comparison. The crack-compliance data are indicated by open and filled symbols and the cut-compliance data are represented by solid and dashed lines. In addition, a stress-intensity factor solution generated using the J-integral [37] method is represented by closed circles in Figure 11. The computationally-determined $K_{residual}$ solution generated using the VCCT technique (open squares in Figures 11 and 12) at various *a*/W values also compare well with experimental data.

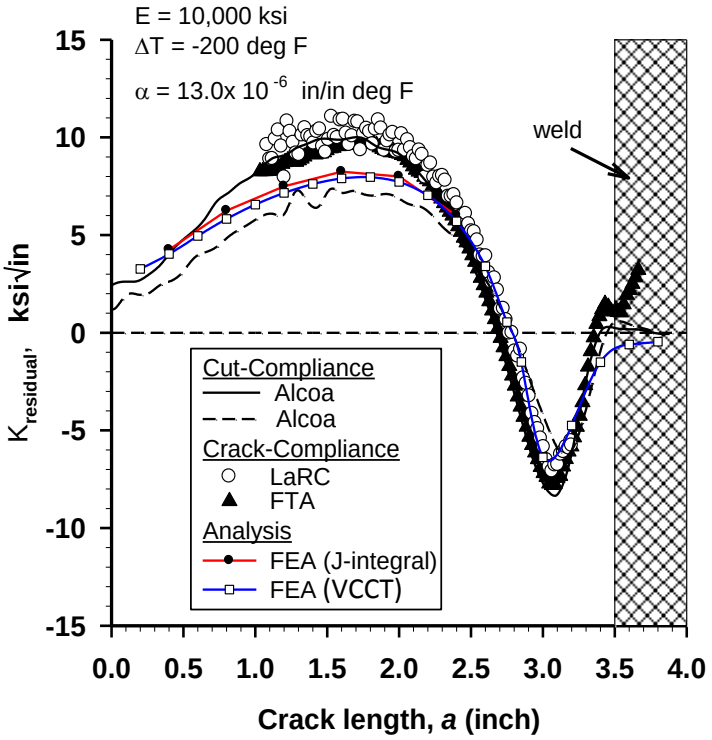

Figure 11 – Residual stress variation for tensile-dominated specimen. Experimental data are shown for comparison.

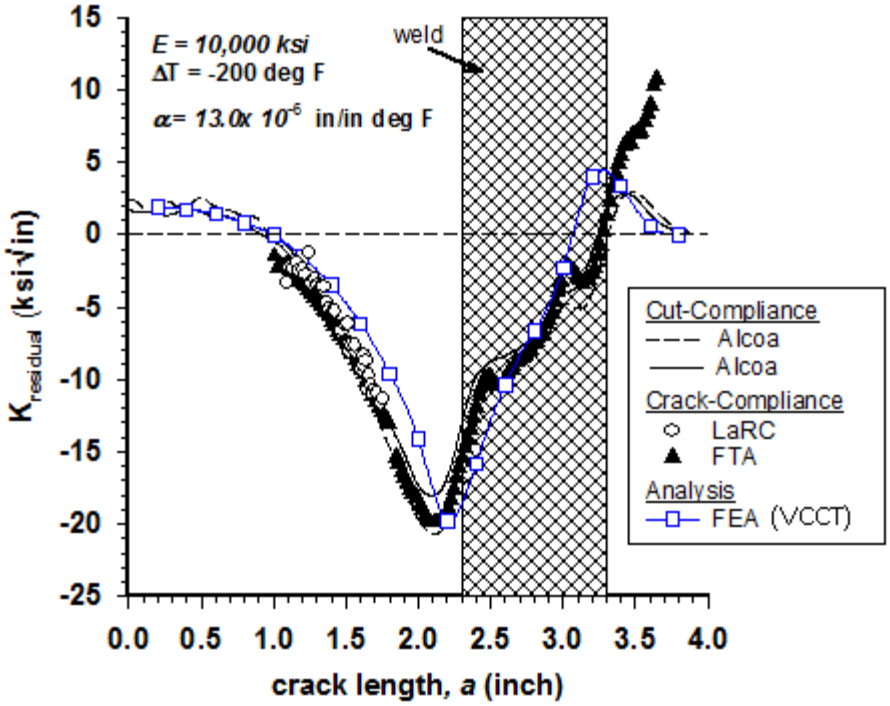

Figure 12 – Residual stress variation for compressive-dominated specimen. Experimental data are shown for comparison.

Discussion

Residual stresses in FSW coupons were determined experimentally using the well-established cut-compliance method and the relatively new crack-compliance method. Both of these test methods produced nearly identical residual stress-intensity factors, an indication that the crack-compliance test method produces valid results and is reproducible in different laboratories. The crack-compliance test has the inherent advantage of being conducted during an ongoing fatigue crack growth test such that fatigue crack growth rate data and residual stress-intensity data are obtained simultaneously. This advantage (over either FCG testing and cut-compliance testing as separate tests) is especially significant in cases where the available material for testing is limited or if significant variation in residual stresses may occur between specimens, such as from a die forging. Consider a scenario where the residual stress field varies between specimens; without crack-compliance testing, one specimen would be used to determine the residual stresses perpendicular to the crack path (cut-compliance) and another would be used to obtain FCG rate data. However, the use of multiple specimens and test methods to characterize the residual-stress-affected crack growth behavior requires specimen-to-specimen consistency in residual stress state. If significant differences in residual stresses exist between specimens, it would be difficult to accurately characterize the effect of residual stress on FCG using data obtained from multiple specimens.

The FSW specimens tested in this study were manufactured with a carefully-controlled welding process such that no significant residual stress differences existed between specimen

types (i.e., all compressive specimens were nearly identical in terms of residual stress field). This observation permitted the constant-K_{tip} tests presented in this paper. Here, the $K_{residual}$ data obtained from a previous test were used to calculate applied loads such that the crack-tip would experience a nearly-constant stress state as the crack propagated across the specimen. This variable-applied-R test resulted in nearly constant crack growth rates, independent of the crack-tip position with respect to the weld and independent of residual stress magnitude and associated $K_{residual}$. Thus, the residual stress was shown to affect the crack tip much as an increase in the (non-cyclic) mean stress whose value varies with the weld-induced residual stress field [38]. This observation allows laboratory results (determined from coupon testing) to be applied to larger structures for prediction of crack growth response.

A computational prediction of the weld-induced residual stress state was made based on thermal contraction/expansion of the weld material. A constant elevated temperature was assigned to the FSW in the absence of residual stress, and residual stresses were generated as the weldment was cooled to ambient conditions. Although the model was simple (linear-elastic material behavior and no variation in ΔT across the weld region) and designed only to capture first-order effects, the predictions were in excellent agreement with the experimental data. The value of ΔT was chosen to match the experimental result for one specimen configuration, and the same value of ΔT was applied to another specimen configuration to predict a residual stress profile. Stress-intensity factors from the predicted profile were found to compare favorably with the experimental results for the original specimen configuration. It is believed that this model input (value of ΔT) is primarily a function of the welding process, thus, coupon testing can be used (along with this modeling approach) to determine the residual stress state of a larger structure. With the combination of this computational approach and coupon test data, it is believed that the FCG response of large structures can be predicted. Specifically, the residual stress field of a complex geometry can be estimated using the equivalent ΔT method, and its effect on fatigue crack growth predicted as an increase in crack-tip mean stress loading. Further study is required to fully validate this premise.

Finally, limitations of load redistribution and linear superposition are continual concerns in the fracture mechanics community. The testing here for the crack-compliance method and the variable-R provide experimental validation for linear superposition, and the results show that the crack-compliance method captures the load redistribution associated with crack growth as long as linear elastic fracture mechanics applies. However, as one might expect, crack-tip plasticity likely can invalidate results when the plastic zone is large relative to the remaining ligament for a given test specimen. Finally, although the crack compliance equation for the $K_{residual}$ calculation is remarkably simple, the sensitivity to data quality is very high. High quality $K_{residual}$ results require significantly better signal quality and algorithmic accuracy than are required for simple compliance crack length determination.

Summary

An experimental and computational study was conducted to determine residual stress effects on fatigue crack growth in aluminum coupons containing friction stir-weld (FSW) induced residual stresses. The effect of residual stress, calculated in terms of its contribution to the crack-tip stress-intensity factor, was obtained using a well-established cut-compliance method and a newly-developed crack-compliance method. Both test methods were found to produce nearly identical $K_{residual}$ results indicating that the new method (crack-compliance) delivers valid and accurate results. The on line crack-compliance method has the advantage of producing both conventional and residual-stress-corrected FCG data from a single test. Moreover, this

method has the ability to partition and remove the residual stress contribution from the FCG test result.

FCG tests were conducted by continuously varying applied loads such that the combination of applied loading and residual stress resulted in constant crack-tip conditions (i.e., the superposition of applied and residual stress components of K is constant). This resulted in nearly constant fatigue crack growth rates, confirming that a constant cyclic crack-tip stress state was achieved, suggesting that the residual stresses affect FCG as a mean stress effect, and confirming linear superposition for the tested conditions (R >0).

A thermal contraction/expansion model has been demonstrated to accurately predict residual stress distributions for specimens containing friction stir welds. Based on the results of the computational model for two configurations of welded coupons, this method is believed to be applicable to the prediction of FCG in welded both small and large structures. Further study is planned to validate this hypothesis.

Finally, the testing here for the crack-compliance method and the variable-R provide experimental validation for linear superposition, and the results show that the crack-compliance method captures the load redistribution associated with crack growth as long as linear elastic fracture mechanics applies.

References

1. Schmidt, H.-J., Voto, C., and Hansson, J., "TANGO Metallic Fuselage Barrel Validation of Advanced Technologies," *Proceedings of the 21st Symposium of the International Committee on Aeronautical Fatigue, ICAF 2001. Design for Durability in the Digital Age, Vol. 1*. J. Rouchon, Ed., Cepadues-Editions, 2001, pp. 273–288.
2. Swift, T., "Widespread Fatigue Damage Monitoring – Issues and Concerns," *Proceedings 5th International Conference on Structural Airworthiness of New and Aging Aircraft*, Hamburg, Germany, 1993, pp. 829-870.
3. Bussu, G. and Irving, P.E., "The Role of Residual Stress and Heat Affected Zone Properties on Fatigue Crack Propagation in Friction Stir Welded 2024-T351 Aluminum Joints," *International Journal of Fatigue*, vol. 25, 2003, pp. 77-88.
4. Hou, C.Y. and Lawrence, V.F., "Crack Closure in Weldments," *Fatigue and Fracture of Engineering Materials and Structures*, vol. 19, 1996, pp. 683-693.
5. Kang, K.J., Song, J.H., and Earmme, Y.Y., "Fatigue Crack Growth through a Tensile Residual Stress Field under Compressive Applied Loading," *Fatigue and Fracture of Engineering Materials and Structures*, vol. 12, 1989, pp. 363-376.
6. Webster, G. A. and Ezeilo, A. N., "Residual Stress Distributions and Their Influence on Fatigue Lifetimes," *International Journal of Fatigue,* vol. 23, 2001, pp. 375–383.
7. Nelson, D. V., "Effects of Residual Stress on Fatigue Crack Propagation," *Residual Stress Effects in Fatigue, ASTM STP 776*, H.S. Reemsnyder, J.F. Throop, Eds., ASTM International, West Conshohocken, PA, 1982, pp. 172–194.
8. Wohlfahrt, H. and Lieurade, H. P., "Influence of Residual Stresses on the Fatigue Strength of Welded Structures," *Handbook on Residual Stresses, Vol. 1,* J. Lu, Ed., 2005, pp. 79–107.
9. Bucci, R.J., "Effect of Residual Stress on Fatigue Crack Growth Rate Measurement," *Fracture Mechanics: Thirteenth Conference, ASTM STP 743*. R. Roberts, Ed., ASTM International, West Conshohocken, PA, 1981, pp. 28-47.

10. Donald, J.K. and Lados, D.A., “An Integrated Methodology for Separating Closure and Residual Stress Effects from Fatigue Crack Growth Rate Data,” *Fatigue and Fracture of Engineering Materials and Structures*, vol. 30, 2006, pp. 223-230.
11. Newman, J.A., Smith, S.W., Seshadri, B.R., Donald, J.K., Blair, A., James, M.A., Bucci, R.J., Brazill, R.L., Schultz, R.W., and Johnston, W.M., “Residual Stress Effects on Fatigue Crack Propagation in a Friction Stir Welded Material,” Residual Stress Summit 2010, Tahoe City, California, September 26-29, 2010.
12. Olson, M.D. and Hill, M.R., “Determination of Residual Stress Intensity Factor in the Compact Tension Coupon,” *Engineering Fracture Mechanics*, vol. 88, 2012, pp. 28-34.
13. ASTM Standard E 647- 08: Standard Test Method for Measurement of Fatigue Crack Growth Rates, *Annual Book of Standards, Vol. 3.01*, ASTM International, West Conshohocken, PA, 2008.
14. Elber, W., “Fatigue Crack Closure under Cyclic Tension,” *Engineering Fracture Mechanics*, vol. 2, 1970, pp. 37-45.
15. Donald, J.K., Bray, G.H., and Bush, R.W., “An Evaluation of the Adjusted Compliance Ratio Technique for Determining the Effective Stress Intensity Factor,” *29th National Symposium on Fatigue and Fracture Mechanics, ASTM STP 1332*, T.L. Panontin and S.D. Sheppard, Eds., ASTM International, West Conshohocken, PA, 1998, pp. 674-695.
16. Zhu, X. K. and Chao, Y. J., “Numerical Simulation of Transient Temperature and Residual Stresses in Friction Stir Welding of 304L Stainless Steel,” *Journal of Materials Processing Technology,* vol. 146, 2004, pp.263–272.
17. Parker, A. P., “Stress Intensity Factors, Crack Profiles, and Fatigue Crack Growth Rates in Residual Stress Fields,” *Residual Stress Effects in Fatigue, ASTM STP 776,* H.S. Reemsnyder, J.F. Throop, Eds., ASTM International, West Conshohocken, PA, 1982*,* pp. 13–31.
18. Wu, S. and Abel, A., “Fatigue Crack Stress Intensity Factors: The Influence of Residual Stresses,” *Proceedings of the Second International Offshore and Polar Engineering Conference*, San Francisco, California, 1992, pp. 312–317.
19. Ge, Y. Z., Sutton, M. A., Deng, X., and Reynolds, A. P., “Limited Weld Residual Stress Measurements in Fatigue Crack Propagation: Part I. Complete Field Representation Through Least Squares Finite-Element Smoothing,” *Fatigue and Fracture of Engineering Materials and Structures,* vol. 29, 2006, pp. 524-536.
20. Sutton, M. A., Reynolds, A. P., Ge, Y.Z. and Deng, X., “Limited Weld Residual Stress Measurements in Fatigue Crack Propagation: Part II. FEM-Based Fatigue Crack Propagation with Complete Residual Stress Fields,” *Fatigue and Fracture of Engineering Materials and Structures,* vol. 29, 2006, pp. 537-545.
21. Spooner, S., “Neutron Residual Stress Measurement in Welds” *Analysis of Residual Stress Using Neutron and Synchrotron Radiation*, M.E. Fitzpatrick and A. Lodini, Eds., Taylor and Francis, London, 2003, pp. 296-318.
22. Liljedahl, C.D.M., Tan, M.L., Zanellato, O., Ganguly, S. Fitzpatrick, M.E., and Edwards, L., “Evolution of Residual Stresses with Fatigue Loading and Subsequent Crack Growth in a Welded Aluminum Alloy Middle Tension Specimen,” *Engineering Fracture Mechanics,* vol. 75, 2008, pp. 3881-3894.
23. Liljedahl, C.D.M., Zanellato, O., Edwards, L., and Fitzpatrick, M.E., “Evolution of Residual Stresses with Fatigue Crack Growth in a Variable Polarity Plasma Arc- Welded Aluminum Alloy Compact Tension Specimen,” *Metallurgical and Materials Transactions A,* vol. 39A, 2008, pp. 2370-2377.
24. Liljedahl, C.D.M., Brouard, J., Zanellato, O., Lin, J., Tan, M.L., Ganguly, S., Irving, P.E., Fitzpatrick, M.E., Zhang, X., and Edwards, L., “Weld Residual Stress Effects on Fatigue Crack Growth Behaviour of Aluminium Alloy 2024-T351,” *International Journal of Fatigue,* vol. 31, 2009, pp. 1081-1088.

25. Hill, M. R. and Nelson, D. V., “The Inherent Strain Method for Residual Stress Determination and Its Application to a Long Welded Joint,” *Structural Integrity of Pressure Vessels, Piping and Components, PVP-Vol. 318*, ASME 1995.
26. DeWald, A. T. and Hill, M. R. “Eigenstrain-based Model for Prediction of Laser Peening Residual Stresses in Arbitrary Three-dimensional Bodies Part 1: Model Description,” *Journal of Strain Analysis for Engineering Design*, vol. 44, 2009, pp. 1-11.
27. Ueda, Y., Fukuda, K., and Kim, Y. C., “New Measuring Method of Axisymmetric Three-dimensional Residual Stresses Using Inherent Strains as Parameters,” *Journal of Engineering Materials and Technology,* vol. 108, 1986 pp. 328–334.
28. Bucci, R. J. , James, M. A., Sklyut, H., Heinimann, M. B., Ball, D. L., and Donald, J. K., "Advances in Testing and Analytical Simulation Methodologies to Support Design and Structural Integrity Assessment of Large, Monolithic Parts," SAE Paper No. 2006-01-3179, 2006 SAE Aerospace Manufacturing and Automated Fastening Conference, De Congrès Pierre Baudis, Toulouse, France, September 12-14, 2006.
29. Schindler, H.J., “Experimental Determination of Crack Closure by the Cut Compliance Technique,” *Advances in Fatigue Crack Closure Measurement and Analysis: Second Volume, ASTM STP 1343*, R.C. McClung and J.C. Newman, Jr., Eds., ASTM International, West Conshohocken, PA, 1999, pp. 175-187.
30. Prime, M. B., “Residual Stress Measurement by Successive Extension of a Slot: The Crack Compliance Method,” *Applied Mechanics Reviews*, vol. 52, 1999, pp. 75-96.
31. Cheng, W., Finnie, I., Gremaud, M., and Prime, M. B., “Measurement of Near Surface Residual Stresses Using Electrical Discharge Wire Machining,” *Journal of Engineering Materials and Technology*, vol. 116, 1994, pp. 1-7.
32. Hill, M. R. and Lin, W. “Residual Stress Measurement in a Ceramic-Metallic Graded Material,” *Journal of Engineering Materials and Technology*, vol. 124, 2002, pp. 185-191.
33. Rankin, J. E., Hill, M. R., and Hackel, L. A., “The Effects of Process Variations on Residual Stress in Laser Peened 7049 T73 Aluminum Alloy,” *Materials Science and Engineering A*, vol. 349, 2003, pp. 279-291.
34. Rybicki, E.F. and Kanninen M.F., “A Finite Element Calculation of Stress Intensity Factors by a Modified Crack Closure Integral,” *Engineering Fracture Mechanics*, vol. 9, 1977, pp. 931–938.
35. Shivakumar, K.N., Tan, P. W., and Newman, Jr., J. C., “A Virtual Crack-Closure Technique for Calculating Stress Intensity Factors for Cracked Three Dimensional Bodies,” *International Journal of Fracture,* vol. 36, 1988, pp. R43–R50.
36. Shivakumar, K.N. and Newman, Jr., J.C., “*ZIP3D- An Elastic-Plastic Finite Element Analysis Program for Cracked Bodies*,” NASA/TM-102753, 1990.
37. Rice, J. R., “A Path Independent Integral and the Approximate Analysis of Strain Concentration by Notches and Cracks,” *Journal of Applied Mechanics*, vol. 35, 1968, pp. 379-386.
38. Riddell, W.T. and Piascik, R.S., “Stress Ratio Effects on Crack Opening Loads and Crack Growth Rates in Aluminum Alloy 2024,” NASA/TM-1998-206929.

REPORT DOCUMENTATION PAGE

Form Approved
OMB No. 0704-0188

1. REPORT DATE *(DD-MM-YYYY)*	2. REPORT TYPE	3. DATES COVERED *(From - To)*
01- 02 - 2015	Technical Memorandum	

4. TITLE AND SUBTITLE

Characterization of Residual Stress Effects on Fatigue Crack Growth of a Friction Stir Welded Aluminum Alloy

5a. CONTRACT NUMBER

5b. GRANT NUMBER

5c. PROGRAM ELEMENT NUMBER

6. AUTHOR(S)

Newman, John A.; Smith, Stephen W.; Seshadri, Banavara R.; James, Mark A.; Brazill, Richard L.; Schultz, Robert W.; Donald, J. Keith; Blair, Amy

5d. PROJECT NUMBER

5e. TASK NUMBER

5f. WORK UNIT NUMBER

432938.11.01.07.43.40.09

7. PERFORMING ORGANIZATION NAME(S) AND ADDRESS(ES)

NASA Langley Research Center
Hampton, VA 23681-2199

8. PERFORMING ORGANIZATION REPORT NUMBER

L-20495

9. SPONSORING/MONITORING AGENCY NAME(S) AND ADDRESS(ES)

National Aeronautics and Space Administration
Washington, DC 20546-0001

10. SPONSOR/MONITOR'S ACRONYM(S)

NASA

11. SPONSOR/MONITOR'S REPORT NUMBER(S)

NASA-TM-2015-218685

12. DISTRIBUTION/AVAILABILITY STATEMENT

Unclassified - Unlimited
Subject Category 26
Availability: NASA STI Program (757) 864-9658

13. SUPPLEMENTARY NOTES

14. ABSTRACT

An on-line compliance-based method to account for residual stress effects in stress-intensity factor and fatigue crack growth property determinations has been evaluated. Residual stress-intensity factor results determined from specimens containing friction stir weld induced residual stresses are presented, and the on-line method results were found to be in excellent agreement with residual stress-intensity factor data obtained using the cut-compliance method. Variable stress-intensity factor tests were designed to demonstrate that a simple superposition model, summing the applied stress-intensity factor with the residual stress-intensity factor, can be used to determine the total crack-tip stress-intensity factor. Finite element, VCCT (virtual crack closure technique), and J-integral analysis methods have been used to characterize weld-induced residual stress using thermal expansion/contraction in the form of an equivalent ¿T (change in local temperature during welding) to simulate the welding process. This equivalent ¿T was established and applied to analyze different specimen configurations to predict residual stress distributions and associated residual stress-intensity factor values. The predictions were found to agree well with experimental results obtained using the crack- and cut-compliance methods.

15. SUBJECT TERMS

Contraction; Crack closure; Fatigue; Friction; Residual concentration; Stress concentration; Thermal expansion; Welding

16. SECURITY CLASSIFICATION OF:			17. LIMITATION OF ABSTRACT	18. NUMBER OF PAGES	19a. NAME OF RESPONSIBLE PERSON
a. REPORT	b. ABSTRACT	c. THIS PAGE			STI Help Desk (email: help@sti.nasa.gov)
					19b. TELEPHONE NUMBER *(Include area code)*
U	U	U	UU	25	(757) 864-9658